

Hydration of chloride anions in the NanC Porin from Escherichia coli: A comparative study by QM/MM and MD simulations

V. Calandrini, J. Dreyer, E. Ippoliti, and P. Carloni

Citation: *The Journal of Chemical Physics* **141**, 22D521 (2014); doi: 10.1063/1.4901111

View online: <http://dx.doi.org/10.1063/1.4901111>

View Table of Contents: <http://scitation.aip.org/content/aip/journal/jcp/141/22?ver=pdfcov>

Published by the [AIP Publishing](#)

Articles you may be interested in

[Comparative study of hydration shell dynamics around a hyperactive antifreeze protein and around ubiquitin](#)
J. Chem. Phys. **141**, 22D529 (2014); 10.1063/1.4902822

[Icosahedral capsid formation by capsomers and short polyions](#)
J. Chem. Phys. **138**, 154901 (2013); 10.1063/1.4799243

[Nonequilibrium molecular dynamics study of electric and low-frequency microwave fields on hen egg white lysozyme](#)
J. Chem. Phys. **131**, 035106 (2009); 10.1063/1.3184794

[Numerical solution of boundary-integral equations for molecular electrostatics](#)
J. Chem. Phys. **130**, 094102 (2009); 10.1063/1.3080769

[Polarizable atomic multipole solutes in a Poisson-Boltzmann continuum](#)
J. Chem. Phys. **126**, 124114 (2007); 10.1063/1.2714528

How can you **REACH 100%**
of researchers at the Top 100
Physical Sciences Universities?
(TIMES HIGHER EDUCATION RANKINGS, 2014)

With *The Journal of Chemical Physics*.

AIP | The Journal of
Chemical Physics

THERE'S POWER IN NUMBERS. Reach the world with AIP Publishing.



Hydration of chloride anions in the NanC Porin from *Escherichia coli*: A comparative study by QM/MM and MD simulations

V. Calandrini,^{1,2} J. Dreyer,^{1,2} E. Ippoliti,^{1,2} and P. Carloni^{1,2,3,a)}

¹Computational Biophysics, German Research School for Simulation Sciences, D-52425 Jülich, Germany

²Institute for Advanced Simulations IAS-5, Computational Biomedicine, Forschungszentrum Jülich, D-52425 Jülich, Germany

³Institute for Neuroscience and Medicine INM-9, Computational Biomedicine, Forschungszentrum Jülich, D-52425 Jülich, Germany

(Received 21 August 2014; accepted 24 October 2014; published online 11 November 2014)

Chloride anions permeate the bacterial NanC porin in physiological processes. Here we present a DFT-based QM/MM study of this porin in the presence of these anions. Comparison is made with classical MD simulations on the same system. In both QM/MM and classical approaches, the anions are almost entirely solvated by water molecules. However, the average water-Cl⁻ distance is significantly larger in the first approach. Polarization effects of protein groups close to Cl⁻ anion are sizeable. These effects might modulate the anion-protein electrostatic interactions, which in turn play a central role for selectivity mechanisms of the channel. © 2014 AIP Publishing LLC. [<http://dx.doi.org/10.1063/1.4901111>]

I. INTRODUCTION

Porins are beta-barrel shaped, bacterial membrane proteins, usually with high content of water molecules. The permeation of physiological anions such as Cl⁻ is a physiologically relevant process.¹ It may involve exchange of water molecules in the coordination shell of the anions as well as replacement of some water molecules with some charged residues of porins and the reverse. Specifically, CHARMM22 force field-based^{2,3} simulations of the OmpF porin have shown that contributions from water molecules and protein atoms to the solvation of the anions vary in a complementary fashion across the porin in order to keep the total solvation of Cl⁻ approximately constant, namely 6–7 atoms.⁴ This is similar to that in bulk solution, where chloride anions have been suggested to be surrounded on average by 7.2 water molecules.⁴ Similarly, in the *N*-acetylneuraminic acid-inducible channel (NanC) porin, AMBER99SB-ILDN-based simulations⁵ have suggested that the average number of water molecules in the solvation shell of Cl⁻ anions varies along the pore between 6 and 7 depending on the protein environment.

Here we re-examine the solvation properties of Cl⁻ anion in one of the investigated porins, the NanC porin, by using hybrid Car-Parrinello quantum mechanics/molecular mechanics (QM/MM) simulations. The starting configurations correspond to anion permeation free energy minima as obtained from previous classical free energy umbrella sampling calculations.⁶ In our QM/MM simulations, the anion and the protein residues surrounding the anion at the different free energy minima positions are treated at the quantum chemical level with density functional theory (DFT), whilst the rest of the protein and the solvent are described by the same empirical force field as that of Ref. 6. Thus, the main difference be-

tween this approach and the previous classical molecular dynamics (MD) simulation is given by the QM description of the chlorine binding sites. This hybrid method has been widely used to study ion permeation in ion channels^{7–9} as well as in a variety of solutes in water, describing water molecules at the classical MM level (see Refs. 10–12 and references therein for a review). The solvation properties of Cl⁻ anion as obtained from QM/MM simulations are compared with those obtained from empirical force field-based simulations. Polarization effects, which might play a crucial role for ion permeation in channels,^{7–9} have been analyzed.

II. METHODS

The setup of the system has been described in our previous publication.⁶ Briefly, the starting structure was based on an X-ray structure of the NanC channel at 1.8 Å resolution (PDB code 2WJR)¹³ with the missing loop L2 added using MODELLER.¹⁴ The porin was embedded in a membrane consisting of 1,2-dioleoyl-*sn*-glycero-3-phosphocholine (DOPC)^{15,16} lipids and surrounded by a water box. Bulk water molecules were substituted by ions to generate a neutral 1.5 M electrolyte solution. The full simulation system consists of the protein monomer embedded in a membrane layer of 254 DOPC molecules with ~16 000 water molecules and about 1000 ions.

From our previous anion permeation free energy calculations based on classical all-atoms umbrella sampling simulations,⁶ we identify three configurations corresponding to two local and the global free energy minima called w67, w79, and w101 in Ref. 6 and Figure 1. They are located in the transmembrane region (TMR) of the porin with *z* ≈ 4.6, 5.2, and 6.3 nm, respectively, along the longitudinal axis *z* of the pore. In these configurations Cl⁻ forms interactions mostly with water molecules, along with some positively charged or polar inner pore residues. Specifically, umbrella sampling

^{a)} Author to whom correspondence should be addressed. Electronic mail: p.carloni@grs-sim.de.

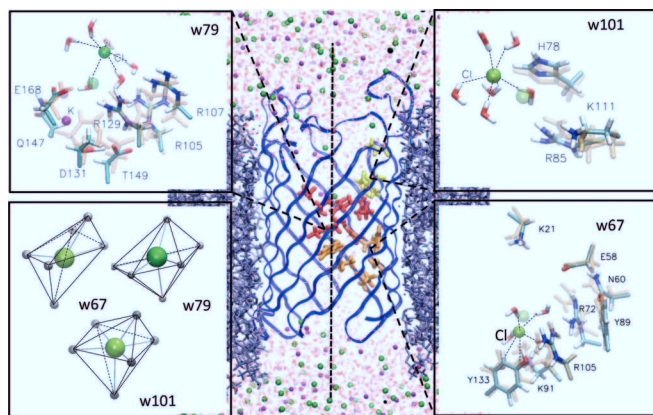


FIG. 1. (Center) Cl^- permeation in the fully solvated NanC porin embedded in a DOPC bilayer. The chloride anions are colored in green. The K^+ cations, present in the simulations, are colored in magenta. The residues in the three binding sites of the Cl^- anions⁶ are colored in yellow, orange, and red. (Side panels) w67, w79, and w101 represent close ups of three anion binding sites⁶ (brown rods). (Colored rods) Correspondent structures from the QM/MM calculations. The water molecules coordinating the anions are shown as well. The left panel at the bottom shows typical distorted octahedral coordination polyhedra of Cl^- (green) extracted from the QM/MM snapshots.

simulations suggest that in w67 the anions are mostly stabilized by residues K91, R72, and R105, in w79 by residues Q147, R105, R129, and R107, and in w101 by R85, K111, and H78. In our QM/MM simulations all of the key residues of each free energy minimum along with the respective anions and some other close residues were treated at the QM level (see Figure 1), while the rest of the system is described at the MM level.

The three systems were subjected to hybrid Car–Parrinello¹⁷ QM/MM simulations.^{18,19} These simulations divided the systems into two parts, a “QM part” and a “MM part.” The QM parts comprise 88, 73, and 37 atoms for w67, w79, and w101, respectively (Figure 1). This part was treated by DFT, with the BLYP recipe for the exchange–correlation functional.^{20,21} The wave function was expanded in a plane-wave basis set up to an energy cutoff of 90 Ry. Only the valence electrons were treated explicitly, while the core electrons were described using norm-conserving pseudopotentials of the Martins–Troullier type.²² The boundaries of the QM part were only chosen in between C–C bonds. An adapted monovalent carbon pseudopotential was employed to saturate the dangling bonds in between the QM and MM regions.²³ Isolated system conditions were imposed in the QM part by employing the Martyna–Tuckerman scheme.²⁴ An empirical van der Waals correction²⁵ provided an inexpensive yet fairly reliable description of London dispersion interactions. The MM part was described by the same force fields employed in previous classical MD simulations,⁶ namely the AMBER99SB-ILDN,⁵ the TIP3P²⁶ model and the parameters by Joung and Cheatham²⁷ for the protein frame, water molecules, and counterions, respectively. The QM and MM parts were coupled using the fully Hamiltonian hierarchical approach.¹⁹ In particular, the electrostatic interactions between the QM and MM parts were explicitly computed for all the classical atoms within a distance of 5.3 Å from any QM atom using a modified Coulomb potential to

prevent electron spill-out.¹⁹ For distances between 5.3 Å and 10.6 Å, the electrostatic interactions were calculated using the D-RESP charge scheme,²⁸ while above a distance of 10.6 Å a multipole expansion scheme was employed.¹⁹ A fictitious electron mass of 600 au and a time step of ~ 0.12 fs were used.

Two thousand steps of annealing were performed to relax the initial structures selected from the previous MD simulations.⁶ Then, the systems were heated up to 310 K by increasing the temperature with a rate of ~ 10 K every 100 steps. Finally, 10 ps-long QM/MM simulations were carried out in an NVT ensemble with constant temperature conditions achieved by using the Nosé–Hoover chain thermostat.^{29–31} The CPMD program combined with the classical MD GRO-MOS96 code,³² through the interface developed by Rothlisberger’s group¹⁹ was employed for the QM/MM simulations.

In order to estimate the polarization effects induced by the anions, we calculated the so-called Wannier Function Centers (WFCs)^{33,34} for the QM part at 0 ps (corresponding to the initial configuration as obtained from classical MD simulations) and at 5 ps along the QM/MM trajectory, with and without the chloride anions.

Classical MD trajectories of 2 ns, whose MD simulation set-up has been described in detail in Ref. 6, are used for comparison with QM/MM approaches. Briefly, the AMBER99SB-ILDN force field⁵ for NanC, the GAFF-based force field³⁵ for DOPC lipids, the TIP3P²⁶ model for water and the parameters by Joung and Cheatham²⁷ for the Cl^- and K^+ ions were used. Periodic boundary conditions were applied and the particle-mesh Ewald (PME) scheme³⁶ was employed to include long-range interactions with a Fourier spacing of 0.1 nm. The cutoff for the real space part of PME and for the van der Waals interactions was set to 1.2 nm. Constant temperature (310 K) and pressure (1 atm) conditions were achieved by coupling the system with a Nosé–Hoover thermostat^{29,30} and the semi-isotropic Rahman–Parrinello barostat,³⁷ respectively.

The coordination number of Cl^- anions at each binding position is calculated by integrating the radial distribution function of the pair Cl^- -H from zero to the first minimum. The comparison with the coordination number obtained by integrating within the same limits the radial distribution function of the pair Cl^- -H_{water} allows one to discriminate whether the coordination shell is composed only of water molecules or of other ligands as well. The average distance between the anion and the hydrogen atoms is obtained from the position of the first maximum of the corresponding radial distribution functions.

The occupancy of the species in the solvation shell of the anion along the trajectories has been calculated using the Hbonds plugin of VMD.³⁸

III. RESULTS AND DISCUSSION

A. Binding sites

The location of Cl^- in the binding site w67 is similar to that obtained by umbrella sampling calculations: The anion position along the pore axis (z-coordinate in Figure 2) fluctuates around a constant value compatible with the chloride

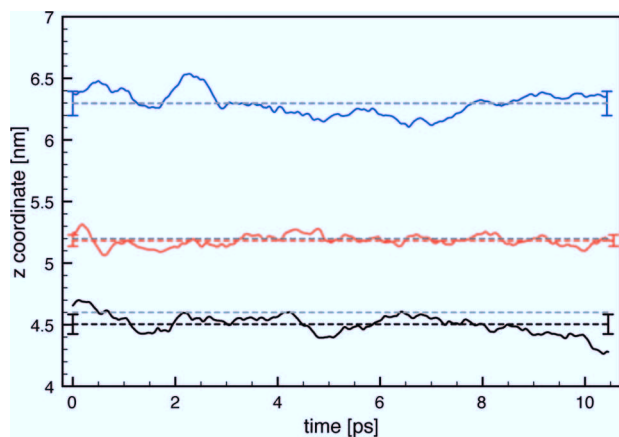


FIG. 2. Positions of the Cl^- anions along the z -axis of the pore (see Fig. 1) during the QM/MM simulations in the w67, w79, and w101 binding sites (black, red, and blue, respectively), plotted as a function of simulated time (colored continuous lines). The average coordinate calculated from the QMMM snapshots are represented as dashed lines. Those from umbrella sampling simulations as gray dashed lines. The corresponding standard deviations are represented by the error bars.

position in the free energy minimum as obtained in previous umbrella sampling calculations within ~ 1 standard deviation (Figure 2). The anion forms hydrogen bonds (H-bonds) to the K91 ammino group (which remains in the anion coordination shell for $\sim 85\%$ of the trajectory length), or, to a much lesser extent, to the R72 guanidinium group (Figure S1 in the supplementary material).⁴¹ It additionally forms on average 5.3 H-bonds with water molecules (see Table I and Figure 3). The typical geometry of the coordination polyhedron corresponds to a distorted octahedron (Figure 1). The Cl^- - H_{water} distance (2.37 \AA) is almost equal to that in bulk water as obtained by previous hybrid QM/MM simulations, yielding 2.35 \AA .¹⁹ Along the 10 ps-long trajectory, the occupancy of the water molecules in the hydration shell of the Cl^- anion ranges from 1 to more than 9 ps.

The Cl^- coordination as obtained by classical MD simulations is similar; on average 5.8 water molecules and the K91 residue (and, to a lesser extent, R72) are H-bonded to the anion, yet the Cl^- -H distances are smaller than in QM/MM simulations (Table I). This of course is to be mainly ascribed to the different level of theory employed. An analysis of the

TABLE I. Chloride H-bonding interactions: Cl^- - H_{total} and Cl^- - H_{water} distances (\AA), along with coordination numbers (CN_{total} and CN_{water}), of the Cl^- anions as obtained from the corresponding radial distribution functions computed from QM/MM and classical MD simulations. The subscript *water* indicates that the analysis is restricted to the water molecules, whilst the subscript *total* to the total number of hydrogen atoms surrounding the anion.

System	Cl^- - H_{total}	First minimum	CN_{total}	Cl^- - H_{water} in channel	CN_{water}
	QM/MMMD			QM/MMMD	
W67	2.37 (1)	3.00(1)	6.4(1)	2.37 (1)	5.3(1)
	2.19 (1)	2.93(1)	6.5(1)	2.20 (1)	5.8(1)
W79	2.44 (1)	3.06(1)	6.5(1)	2.44 (1)	6.3(1)
	2.23 (1)	2.90 (3)	6.0 (1)	2.19 (1)	4.5(1)
W101	2.40 (1)	3.01 (1)	6.7 (1)	2.39 (1)	6.5 (1)
	2.22 (1)	2.95 (1)	6.9 (1)	2.21 (1)	6.7 (1)

occupancy of the water H-bonded to the anion over 10 ps long classical MD trajectories shows the same range in the exchange time-scale of QM/MM simulations. Classical MD simulations of 2 ns show that the occupancy of the water molecule entering solvation shell reaches up to ~ 900 ps with $\sim 20\%$ of the molecules having an occupancy below 10 ps.

Also in the binding site w79, the Cl^- position along the z -axis is similar to that of the MD umbrella sampling calculations (Figure 2). Here, the Cl^- anion is on average coordinated by 6.3 water molecules with an average Cl^- -H distance of $\sim 2.44(1) \text{ \AA}$ (Table I and Figure 3), in a distorted octahedron geometry (Figure 1). Note that this Cl^- -H distance is slightly larger than that in bulk water observed in previous hybrid QM/MM simulations.¹⁹ This can be related to the fact that the anions are far from bulk conditions, being confined inside the channel close to charged binding sites. R105 and, less, R129 replace at times one water H-bond donor, with an occupancy of $\sim 16\%$ and 2% , respectively, of the trajectory length (see Figure S1 in the supplementary material).⁴¹ Also in this case, the Cl^- -H distance derived from QM/MM simulations is larger than that from classical umbrella sampling calculations (Table I). The occupancy of the coordination water over the 10 ps-long QM/MM trajectory ranges from 1 to ~ 8 ps.

The coordination number in classical MD simulations is 6 and typically 1–2 ligands are residues of the protein, namely R129, Q147, or R105, whilst the other ligands are water molecules. (Table I). Classical MD trajectories of 10-ps show that H-bonded water occupancy ranges from 1 to 10 ps, thus suggesting that the ligand exchange timescale is not too different from that observed in QM/MM simulations. In the 2 ns-long classical MD simulations, the occupancy of the water molecules in the solvation shell reaches up to ~ 400 ps with $\sim 20\%$ of the molecules having an occupancy below 10 ps.

In the binding site w101 the position of the Cl^- anion along the porin axis is again compatible with that obtained in the umbrella sampling calculations (Figure 2) within 1 standard deviation. The anion is on average coordinated by 6.7 water molecules with a Cl^- -H distance of $\sim 2.40(1) \text{ \AA}$ (Table I and Figure 3), which is slightly larger than that in bulk water observed in previous hybrid QM/MM simulations,¹⁹ possibly for the same reason discussed before. Occasionally, R85 may enter the coordination shell with occupancy of $\sim 15\%$ of the trajectory length. The occupancy of the water molecules in the coordination shell is similar to that of the binding site w79, ranging from 1 to ~ 8 ps.

The same coordination is qualitatively observed in classical umbrella simulations, although the Cl^- -H distance is significantly smaller (Table I). The occupancy of H-bonded water in 10-ps long classical MD simulations ranges from 1 to ~ 10 ps. Longer 2-ns classical MD simulations show a water occupancy up to ~ 350 ps with $\sim 20\%$ of the molecules having an occupancy up to 10 ps.

B. Polarization effects

Here, we calculate the Wannier Function Centers (WFCs) of the chloride anion binding sites. The WFCs are

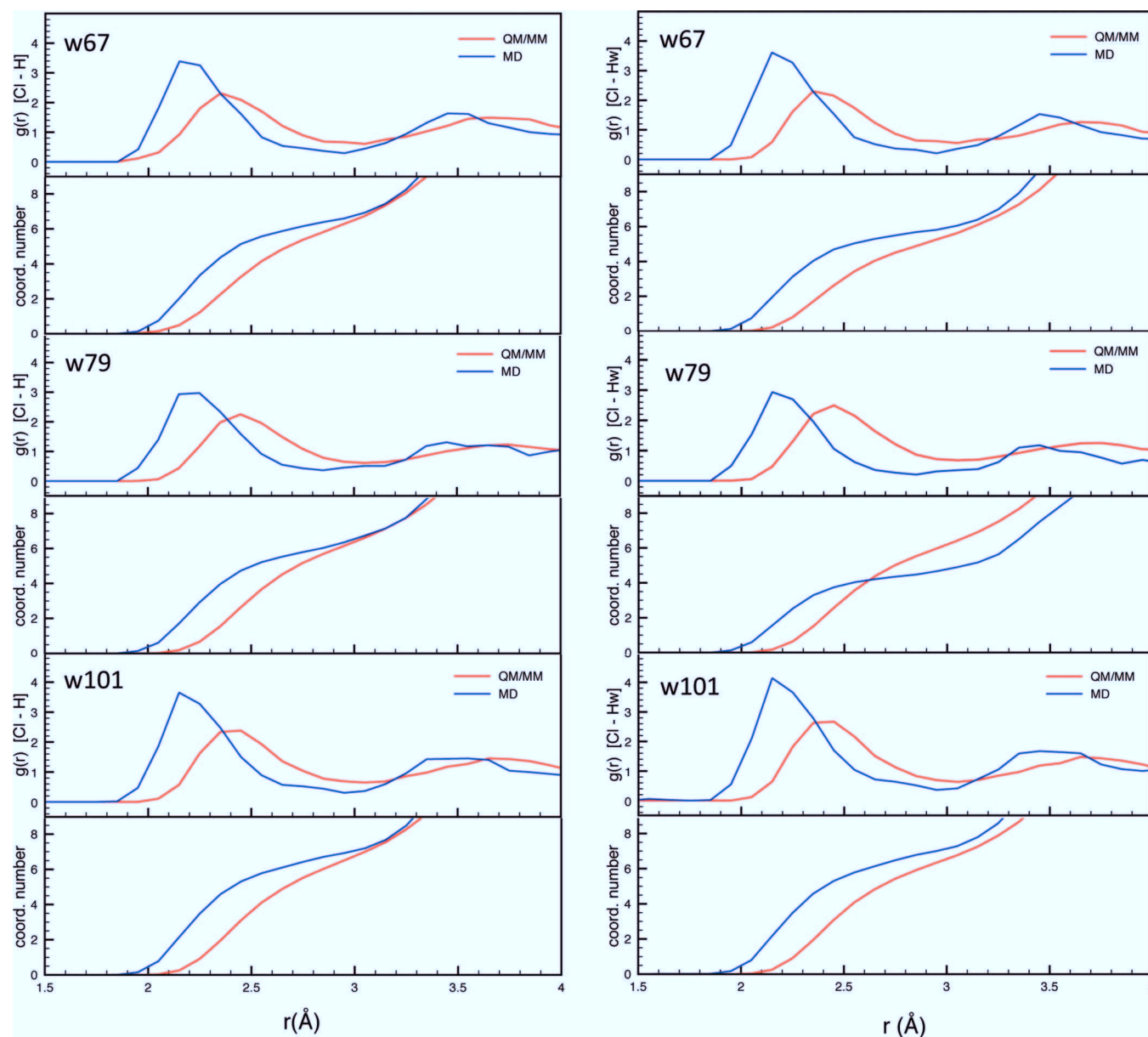


FIG. 3. Radial distribution functions of the pairs Cl^- -H (left column) and Cl^- - H_{water} (right column), and corresponding coordination numbers, as obtained from QM/MM and force field-based MD simulations.

associated with chemical concepts such as electronic lone pairs and chemical bonds.^{33,34} Specifically, we calculate the shifts of WFCs associated with the N-H bonds of amino and guanidinium groups of the porin H-bonding the Cl^- anion or being close to it (Figure 1) both in the presence and in the absence of the chloride anion. For each system, two different configurations, at 0 ps (that is, the starting configuration as obtained from classical umbrella sampling MD) and at 5 ps along the QM/MM simulations, were analyzed.

The only residue forming a stable H-bond with Cl^- anion is K91 in w67. Here, a sizable WFC shift of $\sim 3 \times 10^{-2}$ Å toward the N is observed (Figure 4), which points to a significant modulation of polarity of the N-H bonds induced by the anion. Typical fluctuations at equilibrium of the WFC associated to carbonyl oxygen atoms in biological systems similar to ours range from 5×10^{-3} to 1×10^{-2} Å (see for instance the data reported in Refs. 8 and 39), while the fluctuations of

the WFC associated to the O-H bonds in water are of the order of 2.5×10^{-2} Å (see for instance Ref. 40). Comparison of our values with these data indicates that the WFC displacements induced by the ions on the N-H bonds are sizeable. This suggests that the polarization effects of the chloride ions onto the N-H bonds are rather large.

K and R residues forming water-mediated H-bonds are also polarized in all binding sites. In particular, WFC displacement in the N-H bonds of K side chains of the order of $\sim 4 \times 10^{-3}$ Å are still observed at a distance of ~ 8 Å from the Cl^- anion. Similarly, WFC shifts ranging from $\sim 2 \times 10^{-2}$ Å down to $\sim 6 \times 10^{-3}$ Å are observed for the N-H arginines' guanidinium groups located up to ~ 10 Å away from the Cl^- anion. Obviously, the direction of the displacements along the N-H bonds depends on the orientation of the N-H bonds relative to the Cl^- (see Figure S2 in the supplementary material for details).⁴¹

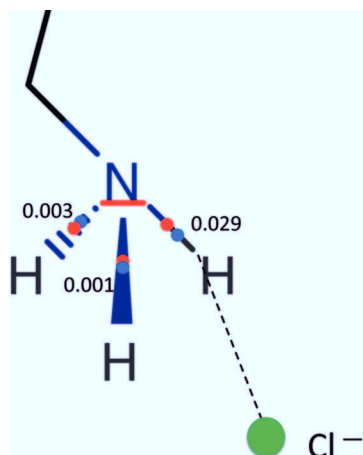


FIG. 4. Illustration of the WFCs of the K91 amino group at ~ 5 ps without (blue points) and with (red points) Cl^- anion in the binding site. The dashed line indicates the hydrogen bond formed with the anion. The numbers are the WFC shifts in Å along the NH bonds, upon Cl^- addition.

IV. CONCLUSIONS

Our data suggest that the QM/MM results are not too dissimilar from those identified by force field calculations. In particular, the anions are either entirely or almost completely solvated in the porin. However, small yet significant differences are found for Cl^- - H_{water} H-bond distances, suggesting that in QM/MM simulations hydration water is less tightly bound to the anion than in classical MD simulations. In addition, the polarization effects induced by the anion on the protein residues are significant. These effects might play an important role in the conduction and/or selectivity mechanisms, which for porins such as NanC is of physiological relevance.

ACKNOWLEDGMENTS

Financial funding from the DFG CA 973/1-1 grant is gratefully acknowledged, as well as computing time granted by the JARA-HPC Vergabegremium (project ID: JARA0054) and provided on the JARA-HPC partition of the RWTH Compute Cluster hosted at Rechenzentrum Aachen.

¹L. N. Csonka, *Microbiol. Rev.* **53**(1), 121–147 (1989).

²D. A. MacKerell, C. L. Brooks, L. Nilsson, B. Roux, Y. Won, and M. Karplus, in *The Encyclopedia of Computational Chemistry*, edited by P. v. R. Schleyer *et al.* (John Wiley & Sons, 1998) Vol. 1, pp. 271–277.

³A. D. MacKerell, D. Bashford, M. Bellott, R. L. Dunbrack, J. D. Evanseck, M. J. Field, S. Fischer, J. Gao, H. Guo, S. Ha, D. Joseph-McCarthy, L. Kuchnir, K. Kuczera, F. T. K. Lau, C. Mattos, S. Michnick, T. Ngo, D. T. Nguyen, B. Prodhom, W. E. Reiher, B. Roux, M. Schlenkerich, J. C. Smith, R. Stote, J. Straub, M. Watanabe, J. Wirkiewicz-Kuczera, D. Yin, and M. Karplus, *J. Phys. Chem. B* **102**(18), 3586–3616 (1998).

⁴W. Im and B. Roux, *J. Mol. Biol.* **319**(5), 1177–1197 (2002).

⁵K. Lindorff-Larsen, S. Piana, K. Palmo, P. Maragakis, J. Klepeis, R. Dror, and D. Shaw, *Proteins: Struct., Funct., Bioinf.* **78**, 1950–1958 (2010).

⁶J. Dreyer, P. Strodel, E. Ippoliti, J. Finnerty, B. Eisenberg, and P. Carloni, *J. Phys. Chem. B* **117**(43), 13534–13542 (2013).

⁷D. Bucher, L. Guidoni, P. Carloni, and U. Rothlisberger, *Biophys. J.* **98**(10), L47–L49 (2010).

⁸D. Bucher, S. Raugei, L. Guidoni, M. D. Peraro, U. Rothlisberger, P. Carloni, and M. L. Klein, *Biophys. Chem.* **124**, 292–301 (2006).

⁹D. Bucher and U. Rothlisberger, *J. Gen. Physiol.* **135**(6), 549–554 (2010).

¹⁰U. Rothlisberger and P. Carloni, in *Computer Simulations in Condensed Matter Systems: From Materials to Chemical Biology* (Springer, 2006), Vol. 704, p. 449.

¹¹P. Carloni, U. Rothlisberger, and M. Parrinello, *Acc. Chem. Res.* **35**(6), 455–464 (2002).

¹²D. Bucher, F. Masson, S. Arey, and U. Rothlisberger, in *Quantum Biochemistry*, edited by C. F. Matta (Wiley-VCH Verlag GmbH & Co. KGaA, Weinheim, Germany, 2010).

¹³C. Wirth, G. Condemine, C. Boiteux, S. Berneche, T. Schirmer, and C. Penef, *J. Mol. Biol.* **394**, 718–731 (2009).

¹⁴A. Fiser and A. Šali, in *Methods in Enzymology*, edited by C. W. Carter, Jr. and M. S. Robert (Academic Press, 2003), Vol. 374, pp. 461–491.

¹⁵R. Vácha, S. W. I. Siu, M. Petrov, R. A. Böckmann, J. Barucha-Kraszewska, P. Jurkiewicz, M. Hof, M. L. Berkowitz, and P. Jungwirth, *J. Phys. Chem. A* **113**(26), 7235–7243 (2009).

¹⁶J. Gordon, J. Myers, T. Foltz, V. Shojia, L. S. Heath, and A. Onufriev, *Nucleic Acids Res.* **33**, W368–W371 (2005).

¹⁷R. Car and M. Parrinello, *Phys. Rev. Lett.* **55**(22), 2471–2474 (1985).

¹⁸E. Ippoliti, J. Dreyer, P. Carloni, and U. Rothlisberger, in *Hierarchical Methods for Dynamics in Complex Molecular Systems*, edited by J. Groten-dorst, G. Sutmann, G. Gompper, and D. Marx (Forschungszentrum Jülich, 2012), pp. 163–182.

¹⁹A. Laio, J. VandeVondele, and U. Rothlisberger, *J. Chem. Phys.* **116**(16), 6941–6947 (2002).

²⁰A. D. Becke, *Phys. Rev. A* **38**(6), 3098–3100 (1988).

²¹C. Lee, W. Yang, and R. G. Parr, *Phys. Rev. B* **37**(2), 785–789 (1988).

²²N. Troullier and J. L. Martins, *Phys. Rev. B* **43**(3), 1993–2006 (1991).

²³O. A. von Lilienfeld, I. Tavernelli, U. Rothlisberger, and D. Sebastiani, *J. Chem. Phys.* **122**(1), 014113 (2005).

²⁴G. J. Martyna and M. E. Tuckerman, *J. Chem. Phys.* **110**(6), 2810–2821 (1999).

²⁵S. Grimme, *J. Comput. Chem.* **25**(12), 1463–1473 (2004).

²⁶W. L. Jorgensen, J. Chandrasekhar, J. D. Madura, R. W. Impey, and M. L. Klein, *J. Chem. Phys.* **79**(2), 926–935 (1983).

²⁷I. Joung and T. Cheatham, *J. Phys. Chem. B* **112**, 9020–9041 (2008).

²⁸A. Laio, J. VandeVondele, and U. Rothlisberger, *J. Phys. Chem. B* **106**(29), 7300–7307 (2002).

²⁹S. Nose, *Mol. Phys.* **52**(2), 255–268 (1984).

³⁰W. G. Hoover, *Phys. Rev. A* **31**, 1695–1697 (1985).

³¹G. J. Martyna, M. L. Klein, and M. Tuckerman, *J. Chem. Phys.* **97**(4), 2635 (1992).

³²W. F. van Gunsteren, S. R. Billeter, A. A. Eising, P. H. Hünenberger, P. Krüger, A. E. Mark, W. R. P. Scott, and I. G. Tironi, *Biomolecular Simulation: The GROMOS96 Manual and User Guide* (Vdf Hochschulverlag AG an der ETH Zürich, Zürich, Switzerland, 1996).

³³N. Marzari, A. A. Mostofi, J. R. Yates, I. Souza, and D. Vanderbilt, *Rev. Mod. Phys.* **84**(4), 1419–1475 (2012).

³⁴N. Marzari and D. Vanderbilt, *Phys. Rev. B* **56**(20), 12847–12865 (1997).

³⁵S. Siu, R. Vácha, P. Jungwirth, and R. Böckmann, *J. Chem. Phys.* **128**, 125103 (2008).

³⁶U. Essmann, L. Perera, M. L. Berkowitz, T. Darden, H. Lee, and L. G. Pedersen, *J. Chem. Phys.* **103**(19), 8577–8593 (1995).

³⁷M. Parrinello and A. Rahman, *J. Appl. Phys.* **52**(12), 7182–7190 (1981).

³⁸W. Humphrey, A. Dalke, and K. Schulten, *J. Mol. Graphics* **14**, 33–38 (1996).

³⁹L. Guidoni and P. Carloni, *Biochim. Biophys. Acta* **1563**(1–2), 1–6 (2002).

⁴⁰A. Hassanali, M. K. Prakash, H. Eshet, and M. Parrinello, *Proc. Natl. Acad. Sci. U.S.A.* **108**(51), 20410–20415 (2011).

⁴¹See supplementary material at <http://dx.doi.org/10.1063/1.4901111> for the structural determinants of the binding sites and for the Wannier Function Centers (WFCs) displacements along N–H bonds in the guanidinium groups of the R residues and in the amino groups of the K residues in the binding sites.